Remote Sens. **2015**, *7*, 6535-6557; doi:10.3390/rs70606535

OPEN ACCESS

remote sensing

ISSN 2072-4292

www.mdpi.com/journal/remotesensing

Article

Rapid Assessment of Crop Status: An Application of MODIS and SAR Data to Rice Areas in Leyte, Philippines Affected by Typhoon Haiyan

Mirco Boschetti [1,*], Andrew Nelson [2,*], Francesco Nutini [1], Giacinto Manfron [1], Lorenzo Busetto [1], Massimo Barbieri [3], Alice Laborte [2], Jeny Raviz [2], Francesco Holecz [3], Mary Rose O. Mabalay [4], Alfie P. Bacong [4] and Eduardo Jimmy P. Quilang [4]

[1] Institute for Electromagnetic Sensing of the Environment, Italian National Research Council, Via Bassini 15, Milan 20133, Italy; E-Mails: nutini.f@irea.cnr.it (F.N.); manfron.g@irea.cnr.it (G.M.); busetto.l@irea.cnr.it (L.B.)

[2] International Rice Research Institute (IRRI), Los Baños, Laguna 4031, Philippines; E-Mails: a.g.laborte@irri.org (A.L.); j.raviz@irri.org (J.R.)

[3] Sarmap, Cascine di Barico 10, Purasca 6989, Switzerland; E-Mails: mbarbieri@sarmap.ch (M.B.); fholecz@sarmap.ch (F.H.)

[4] Philippine Rice Research Institute (PhilRice), Muñoz, Nueva Ecija 3119, Philippines; E-Mails: mro.mabalay@philrice.gov.ph (M.R.O.M.); alfiebacong@yahoo.com.ph (A.P.B.); ejp.quilang@philrice.gov.ph (E.J.P.Q.)

***** Authors to whom correspondence should be addressed; E-Mails: boschetti.m@irea.cnr.it (M.B.); a.nelson@irri.org (A.N.); Tel.: +09-2-2369-9297 (M.B.); +63-2-580-5600 (ext. 2592) (A.N.).

Academic Editors: Tao Cheng, Clement Atzberger and Prasad S. Thenkabail

Received: 17 March 2015 / Accepted: 13 May 2015 / Published: 26 May 2015

Abstract: Asian countries strongly depend on rice production for food security. The major rice-growing season (June to October) is highly exposed to the risk of tropical storm related damage. Unbiased and transparent approaches to assess the risk of rice crop damage are essential to support mitigation and disaster response strategies in the region. This study describes and demonstrates a method for rapid, pre-event crop status assessment. The *ex-post* test case is Typhoon Haiyan and its impact on the rice crop in Leyte Province in the Philippines. A synthetic aperture radar (SAR) derived rice area map was used to delineate the area at risk while crop status at the moment of typhoon landfall was estimated from specific time series analysis of Moderate Resolution Imaging Spectroradiometer (MODIS) data. A spatially explicit indicator of risk of standing crop loss was calculated as the time

between estimated heading date and typhoon occurrence. Results of the analysis of pre- and post-event SAR images showed that 6500 ha were flooded in northeastern Leyte. This area was also the region most at risk to storm related crop damage due to late establishment of rice. Estimates highlight that about 700 ha of rice (71% of which was in northeastern Leyte) had not reached maturity at the time of the typhoon event and a further 8400 ha (84% of which was in northeastern Leyte) were likely to be not yet harvested. We demonstrated that the proposed approach can provide pre-event, in-season information on the status of rice and other field crops and the risk of damage posed by tropical storms.

Keywords: phenology; typhoon; rice; Philippines; rapid damage assessments

1. Introduction

1.1. Rice Crops in Asia and Their Exposure to Tropical Storms

Rice is the only staple crop suited to humid, high rainfall environments. Rice is predominantly grown in regions and seasons in Asia that are highly prone to extreme weather events such as tropical storms (called Typhoons in the northwestern Pacific ocean; Tropical Cyclones in the Indian, southwest Pacific and southern Atlantic oceans, and; Hurricanes in the northern Atlantic and northern Pacific oceans).

Figure 1 shows the approximate area occupied by standing rice crops in Asia for every month of the year, based on crop calendars [1] and national statistics [2]. About 70% of the region's rice is grown in the monsoon season from June to October, reaching a peak of almost 100 million hectares in August [1]. The same figure also shows the average monthly frequency of tropical storms in the Western Pacific between 1959 and 2011 [3]. There is a striking correlation suggesting that the main rice crop season in Asia is highly exposed to the risk of storm-related damage.

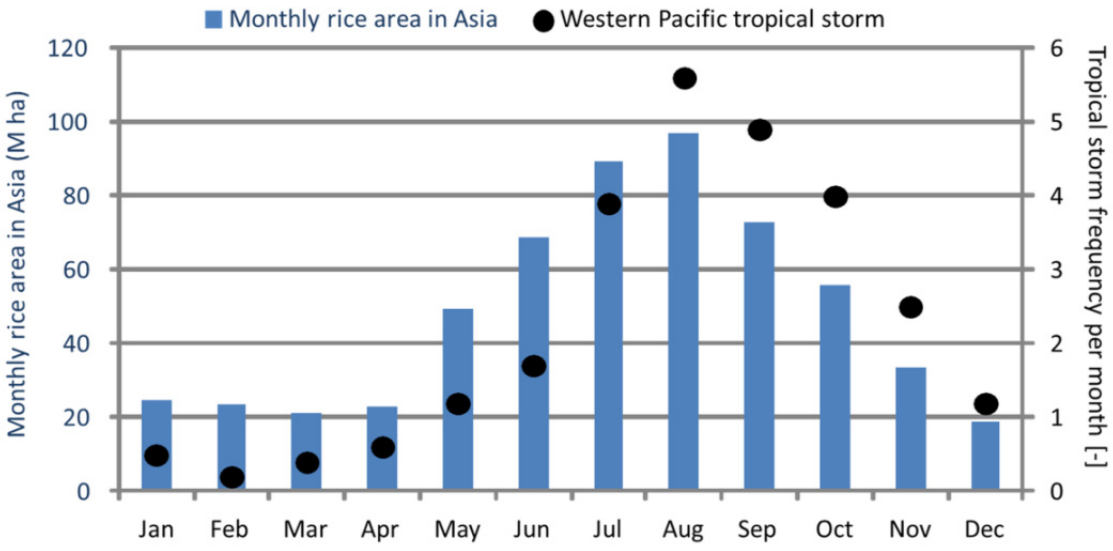

Figure 1. Monthly rice area (M ha) in Asia *vs*. average number of tropical storms per month in the western Pacific between 1959 and 2011.

Cyclones make landfall in eastern India, Bangladesh and Myanmar, while typhoons affect the Philippines, Vietnam, southern and eastern China, Taiwan and Japan. Specifically, the most vulnerable areas are the insular region of Southeast Asia and the coastal areas of mainland Asian countries (although severe storms can affect inland areas too) since significant amounts of rice are produced in floodplains, deltas and other low lying areas in coastal regions. Storm related crop losses in the main growing season can have significant negative impacts on rice production, imports, exports, and prices. Inevitably, these have a disproportionately high impact on the more vulnerable sectors of society, which depend on rice for a substantial proportion of their income (producers) and calories (consumers).

1.2. Typhoon Haiyan and Its Impact in Philippines

The Philippines in particular is affected by an average of 20 tropical storms every year, some of which develop into devastating typhoons. Typhoon Haiyan (also called Typhoon Yolanda in the Philippines) developed into a category five 'super-typhoon' shortly before it made landfall on the eastern Visayas on the 8 November 2013. The eye of the typhoon passed directly over Leyte and its capital city of Tacloban as the typhoon moved from the Western Pacific across the Philippines and then into the South China Sea by the 9 November. The resulting devastation from sustained winds of up to 230 km/h, widespread flooding and the 5–6 m storm surge were well documented in the following weeks and months.

From official reports, casualties in the country reached over 6000 with over 1000 still missing two months after the typhoon [4]. More than 3.4 million families were affected, with nearly a million displaced in 44 provinces in the country. Of the total casualties in the country, 86% were from the province of Leyte. Total cost of damages was estimated at 39.8 Billion (B) Pesos (0.9B USD) and nearly one-fourth were damages to crops including rice and corn. In Leyte, cost of damages to agriculture and infrastructure was estimated at 6.8B Pesos (154M USD) with 1.4B Pesos (32M USD) of damage to rice and corn crops in the province.

1.3. Assessing the Risk of Crop Damage and Actual Crop Damage from Tropical Storms

Tropical storms can affect thousands of hectares of crop at any time during the main rice-growing season. Mitigation and disaster response strategies related to food security require pre- and post-event information on the likely impact and actual impact on crops in the path of a tropical storm.

Accurate information pre-event can assist decision-makers to take appropriate actions to safeguard recently harvested crops or to advance the harvest period so that crops are removed from the field in time. Pre-event assessments would need to be part of routine crop information collection procedures and may not be a high priority for local agricultural officers with many competing demands on their resources. Accurate information post-event can help to assess damages more accurately and determine appropriate compensation, as this is directly linked to inputs and investments such as seeds, fertilizers and labor which will vary depending on the crop stage at time of loss. Post-event assessments can be challenging if access to the area is limited or dangerous. Furthermore, there are often conflicting reports from different agencies and media outlets and there can be pressure for local offices to inflate damage reports to secure greater emergency assistance.

Thus, there is a need to provide unbiased and timely estimates of crop status with sufficient lead-time for agencies and governments to act upon this information. There are several examples of the

use of remote sensing to provide such information, which we briefly review below. We focus on examples and applications in Asia related to flooding from extreme or prolonged rainfall, storm surges or tsunamis—all of which can result in submergence related damages to crops.

1.4. Remote Sensing as a Source of Unbiased and Timely Information on Crop and Vegetation Status

Affected areas can be identified and damages from floods or tropical storms can be evaluated using multi-temporal satellite imagery (both optical and radar), analysis of ancillary spatial data and ground based reporting [5]. Also, non-authoritative data, such as volunteered geographical data (sourced from online video, photos and social media streams *etc.*) and crowd sourced data (e.g., voluntary photo interpretation of aerial images), have been used to provide additional information that is integrated with authoritative data (from agencies mandated to collect such information), in order to perform flood impact assessments [6].

There are several examples of the use of remote sensing and spatial data to assess post-event impact [7–9]. Chau *et al.*, [9] assessed the potential impacts of extreme floods on agriculture in Vietnam by overlaying historical flood inundation maps (produced from flood depth markers recorded for each past flood event) and land use maps. This form of assessment results in risk maps that evaluate the potential impact on natural resources, which, in turn, aids planning activities. However, when an extreme event occurs, it is also important to have a rapid—and if possible a pre-event—estimation of actual agricultural area and actual crop growth stages that would complement such risk maps.

Geospatial and remote sensing based damage assessments have been used in post-tsunami impact assessments (e.g., [10,11]). On 26 December 2004, earthquakes in the Indian Ocean triggered massive waves that caused vast destruction of many coastal areas in the region [12]. This well documented and tragic event massively impacted coastal areas on both sides of the Indian Ocean, from Indonesia to Sri Lanka, and resulted in significant loss of lives, damaged coastal infrastructure and flooding. Some of these impacts were documented through geospatial information. Specific examples include the use of high-resolution imagery (IKONOS satellite datasets) to map changes in vegetation near Aceh, Indonesia, immediately after the event [13], mapping of coastal vegetation changes in Phang Nga province, Thailand [14,15] and assessments of the protection potential of mangrove vegetation cover along the west coast of Thailand [16]. ASTER/Landsat imagery has been used to estimate tsunami-damaged areas [12] and to map and assess vegetation changes—using vegetation indices such as the Normalized Difference Vegetation Index (NDVI)—due to short-term [11] and long-term tsunami effects [17]. These studies are extremely useful for estimating the damages to natural resources. They can support rehabilitation, help to prioritize interventions and draw attention to the impact of these events in a visually compelling and quantitative manner. However, the direct and rapid evaluation of the crop losses incurred in the current season was not the aim of these studies.

In response to Typhoon Haiyan, the Food and Agriculture Organization (FAO) collected and published available information on the impact of the typhoon on the Philippines. A map with an assessment of the damages was provided in their report [18], but this did not include an assessment of the crop condition at the time of the event.

All of the above approaches are reactive and take place post-event. Figure 2 shows the general timeframe of post-event remote sensing assessments. Once an event occurs, pre-event information on

land cover and archives of earth observation (EO) imagery are compared to EO images acquired post-event, any changes are detected and summarized through spatial analysis.

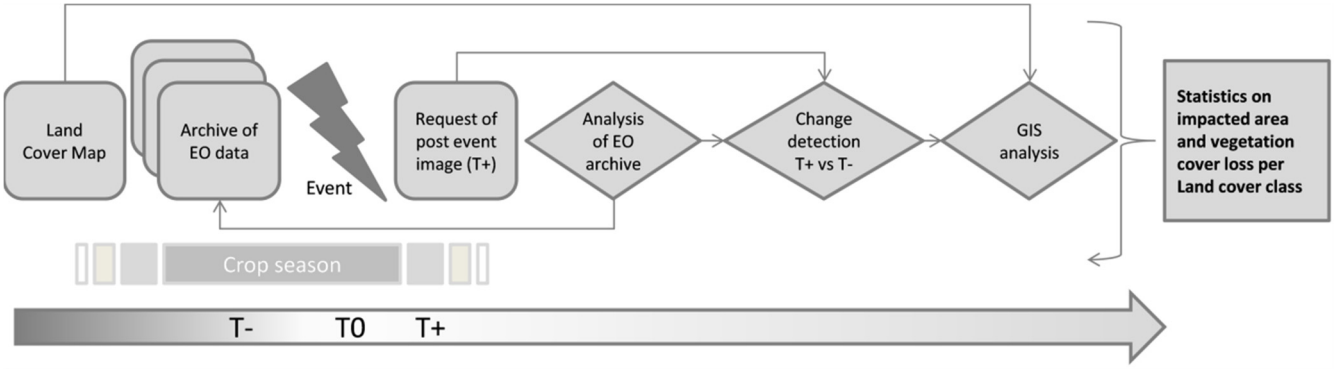

Figure 2. The timeline of post-event remote sensing assessments.

As outlined in Section 1.3 there is a need to complement this approach with a more proactive approach to crop information to assess the risk of damage before the event takes place. Our aim in this study is to develop and demonstrate a methodology that can provide near real time information on the likely impact of a specific event.

1.5. A Remote Sensing-based Proposal for a Proactive Approach on Rice Crop Status Assessment

There are two conditions that need to be met to deliver such near real time information [19]. First, there must be a high spatial resolution rice crop area map of the location and season at risk. Second, there must be a suitable source of timely, high temporal resolution remote sensing information that can be analyzed to provide accurate information on the current rice crop status within that mapped area [20,21]. Availability of these two complementary layers of remote sensing information can be exploited to derive spatially explicit estimates of crop status. This information can be related to the predicted or observed date of a tropical storm event, for immediate damage mitigation strategies or post-event damage estimation. Alternatively, it can be used to assess the frequency of exposure to storms at different crop growth stages and hence develop longer term mitigation strategies such as growing shorter duration varieties, choosing earlier/later planting windows, or adopting alternative crop rotations/land use.

Figure 3 shows the general timeframe of this pre-event (proactive) approach combined with a post-event (reactive) approach. As in Figure 2, a crop map (or land cover map), a pre-event image and a post event image are acquired and analyzed reactively to assess the actual damage after the event. The proactive information comes from the crop map and continual analysis of high temporal information on the crop status, analyzed before the event to assess the risk of damage to the standing crop. The two approaches are complementary.

In this study, we propose a proactive crop status assessment method that can provide near real time information on the likely impact of a specific event. We apply *ex-post* in parallel with a reactive damage assessment for the case of Typhoon Haiyan and its impact on the rice growing areas of Leyte province, Philippines. We first describe the study site, our data (Section 2) and methodology (Section 3). The results section (Section 4) assesses the derived remotely sensed information on crop status/growth stage

at the time of the event and compares these estimates to available field data. Finally, we discuss the significance of the results and the potentials of the proposed approach within the framework of planned operational satellite missions.

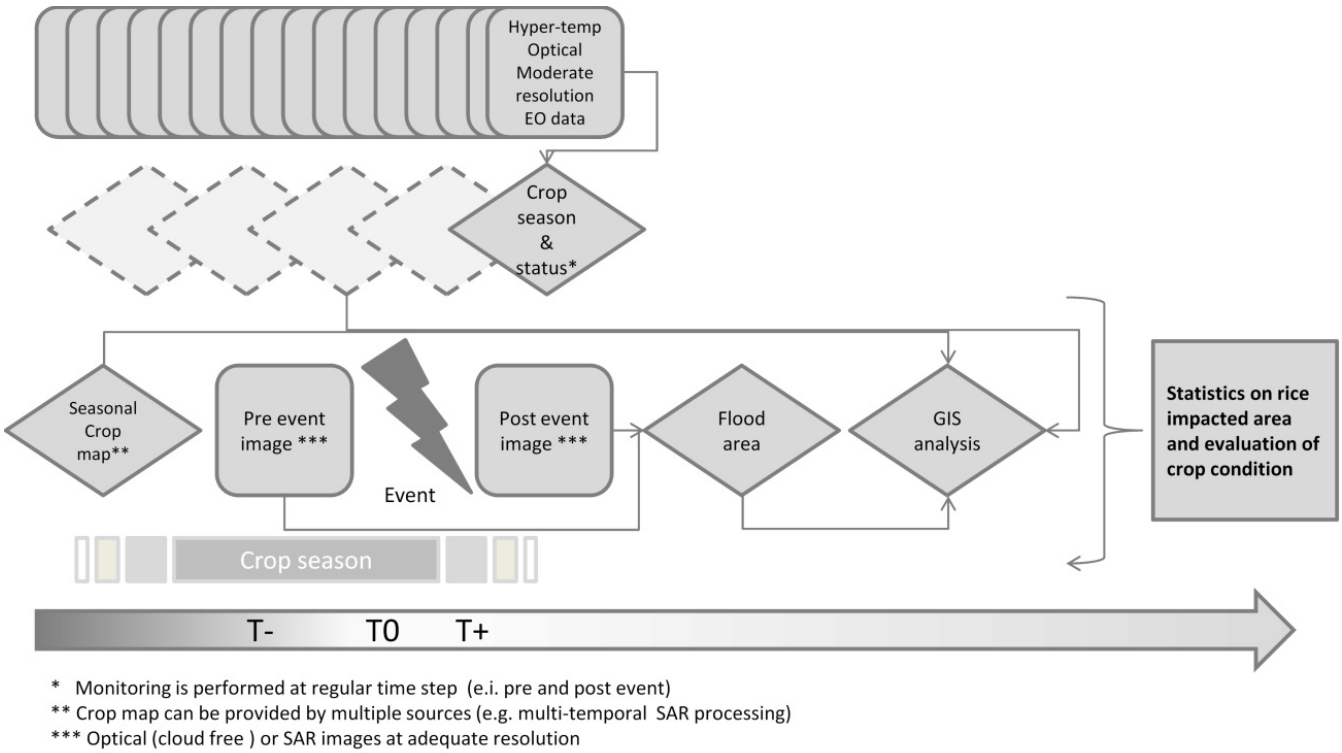

Figure 3. A combined proactive and reactive remote sensing approach to evaluate the risk of crop losses and the actual crop losses due to flooding from tropical storms.

2. Study Site and Data

2.1. Leyte Province and Its Rice Production Systems

Leyte is a province in the eastern part of the Visayas island group of the Philippines. The study site is the northern part of Leyte, which was the most strongly affected by Typhoon Haiyan. Figure 4 shows the study site, the typhoon track and rice cultivated area during the 2013 wet season (July to December) (from [22]). The source and generation of the rice area map are described in Section 3.

Leyte has a tropical climate with regular rainfall through the year. Poverty incidence is high (31% in 2012 [23]). Rice is cultivated on the east and west coasts of the island, while the hilly central area is occupied mainly by forests. The total rice area in the province in 2012 was 133000 hectares, 65% of which is irrigated [24]. Most farmers establish their crop by transplanting 21-day old seedlings. Popular varieties include NSIC Rc-222, NSIC Rc-238 and NSIC Rc-216, which are inbred varieties with durations ranging from 110 to 114 days.

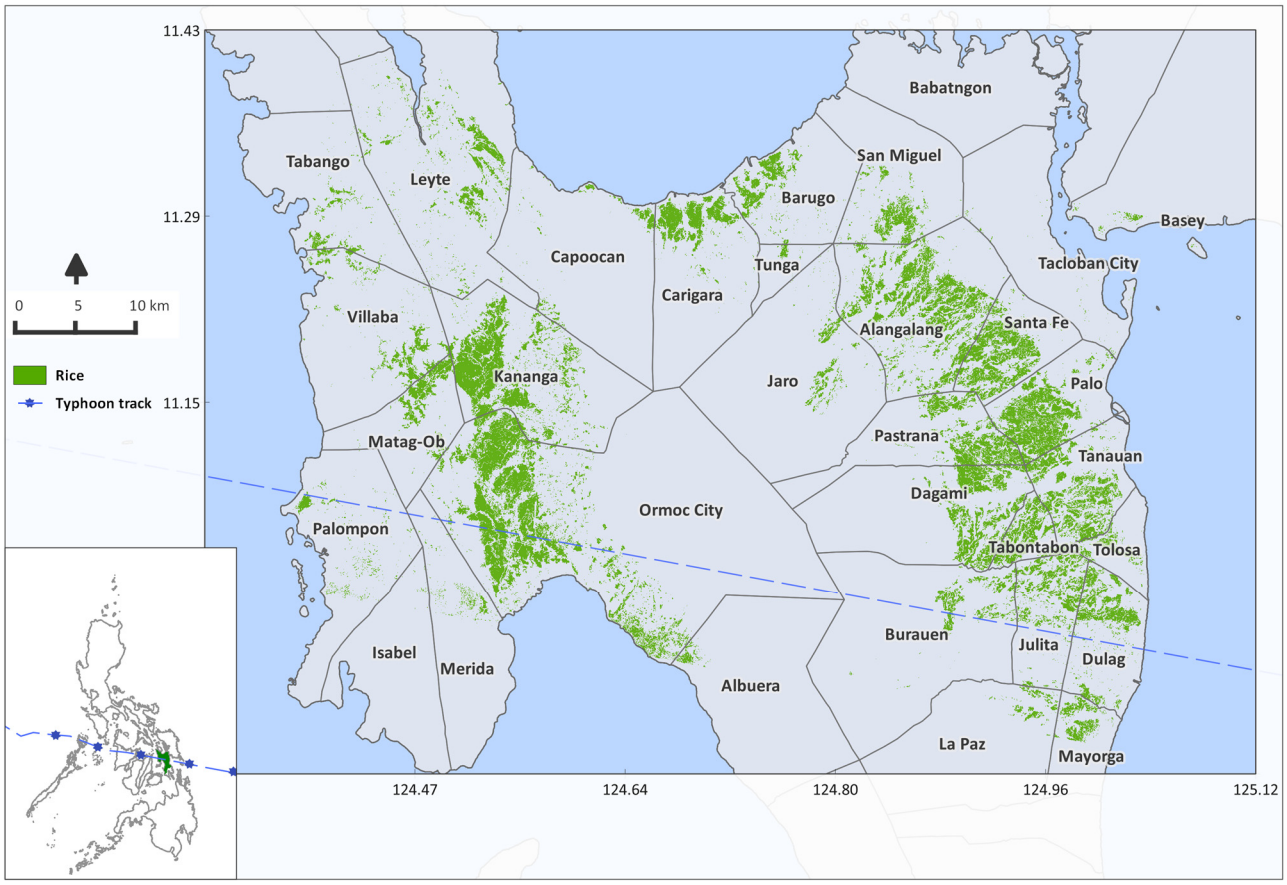

Figure 4. Northeastern part of Leyte Province. Wet season rice area in green, track of typhoon Haiyan in blue, municipal boundaries in black. Inset map shows the location of Leyte in the Philippines.

Rice is grown in two distinct seasons per year and here we focus on the main or wet season. The transplanting window for the wet season in this region spans several months with farmers establishing their crop anytime between May and August, though the peak transplanting month is June. Such a large range in transplanting dates over a small area reinforces the need for a method that can provide spatial and temporal information on crop status. Since the dominant varieties mature in approximately four months, harvesting takes place between September and December, peaking in October and November.

2.2. Remote Sensing Data

Two sources of Earth Observation (EO) data were used to perform the analysis (Table 1). Very High Resolution (VHR, 3 m) synthetic aperture radar (SAR) data were used to map (i) rice cultivated areas in the 2013 wet season and (ii) post-typhoon flooded areas, while multi-temporal Moderate Resolution (MR, 250 m) optical data were used to assess crop seasonality and crop growth stage at the time of the typhoon event.

Cultivated rice area of the 2013 wet season was produced by analyzing multi-temporal Cosmo-SkyMed (CSK) data acquired every 16 days from 15 May to 20 September 2013, as described in [22].

Table 1. EO data exploited in the analysis.

Location	Northwest Leyte	Northeast Leyte	Northeast Leyte		Leyte
Purpose	Rice area map	Rice area map	Flooded area detection		Rice crop status
Satellite or instrument	Cosmo-SkyMed (CSK 1, 3 and 4)	Cosmo-SkyMed (CSK 1 and 4)	Cosmo-SkyMed (CSK 1 and 2)		Terra and Aqua
Sensor mode	Stripmap	Stripmap	Stripmap		MODIS
Product	SLC	SLC	SLC		MOD13Q1 and MYD13Q1
Band	X (3.12 cm)	X (3.12 cm)	X (3.12 cm)		Red (620–670 nm), NIR (841–876 nm), Blue (459–479 nm)
Resolution (m)	3	3	3		250
Swath (km)	40 × 40	40 × 40	40 × 40	40 × 40	1200 × 1200
Scene center	11.18°N 124.56°E	11.11°N 124.89°E	11.11°N 124.89°E	11.08°N 124.93°E	14.9° N 129.41° E
Polarization	HH	HH	HH	HH	-
Look	Right	Right	Right	Right	-
Orbit	Descending	Descending	Descending	Descending	Descending
Incidence angle	48	46	46	54	-
Cycle (days)	16	16	-	-	16 (8)
Start day	12 May 2013	15 May 2013	20 September 2013	8 November 2013	6 December 2012
End day	24 September 2013	20 September 2013	11 November 2013	16 November 2013	11 December 2013
Images	9	10	2	2	70

Flooded area was analyzed only for northeast Leyte because it was the area where the typhoon first made landfall and was expected to be the area most heavily affected by the typhoon. Where possible, flood assessments should rely on identical sources of pre- and post-event imagery, but a rapid post-event image depends on the orbit frequency of the satellite. Fortunately, most SAR platforms have the ability to change the viewing angle to allow nearby orbits to observe the required area. We acquired flood assessment post-event CSK image with the same acquisition geometry as the May–September data stack on 11 November 2013 and two CSK images with a different viewing angle on 8 and 16 November 2013. Footprints of the SAR data are provided in the supplementary materials (Supplementary Figure S1).

We used the MOD13Q1 (Terra satellite) and MYD13Q1 (Aqua satellite) 250 m resolution vegetation indices products available for Leyte from December 2012 to December 2013. These data are free to download from the USGS Land Processes Distributed Active Archive Centre (LP DAAC) [25]. For both sensors, these data are provided as 16-day composites with an 8 days nominal shift (Terra 16-day composites start at the day of the year (DOY) 001, while the Aqua compositing period starts at DOY 009). MOD/MYD13Q1 products are developed using the Constrained View Angle-Maximum value Composite (CV-MVC). Seventy composites (35 each for MOD13Q1 and MYD13Q1 products) were

downloaded to analyze the entire 2013 crop year, and used to create a synthetic 8-day time series exploiting the nominal composite date to create a temporal series [26].

2.3. Field Data and Additional Spatial Information

Ground data were available as described in [22]. These data were specifically acquired to support the analysis of Very High Resolution SAR data. Field observations were performed throughout the 2013 wet season in 40 paddy fields in northwest and northeast Leyte (20 parcels within each CSK footprint) across eight municipalities. These fields were selected, with the farmers' consent, prior to the start of the rice growing season and the SAR image acquisition schedule. Observations were conducted on (or as close as possible to) the image acquisition date, using a standardized protocol. Observations included latitude and longitude from handheld GPS receivers, descriptions and photos of the status of the field, plant height, water depth, weather conditions and crop growth stage. At the end of the season, farmers were also interviewed to collect information on the rice variety, water source, crop management and establishment practices, and inputs such as pesticides and fertilizers. A total of 400 field observations were made through the season.

A further 184 validation points were collected in the same footprints for rice map accuracy assessment as described in [22].

Administrative municipal boundaries used in aggregating results were obtained from the Global Administrative Areas Database (GADM) [27].

3. Methods

We first describe the analysis and derived information from the proactive assessment and briefly describe the same for the reactive assessment although there are common inputs used in both.

3.1. Proactive Assessment of Rice Crop Status and Risk of Damage

The proactive assessment describes the pre-event status of the crop using processed MODIS time series data to estimate key rice crop stages within a predefined rice crop mask derived from SAR data (see Section 3.1.1 and 3.1.4 for the crop mask). The SAR data and MODIS time series data were processed as follows.

3.1.1. Rice Crop Mask from SAR Data

A fully automated processing chain was developed to convert the multi-temporal space-borne SAR Single Look Complex (SLC) data into terrain-geocoded σ^0 values. Then, a multi-temporal σ^0 rule-based rice detection algorithm was applied to the time series using thresholds derived from 40 in-season monitoring locations within the two SAR footprints where monitoring took place. A confusion matrix was used to estimate the classification accuracy of the rice maps based on observed field data from 184 locations in rice and non-rice areas. The resulting maps show the detected rice area for the 2013 wet season and were estimated to have a classification accuracy of 87% for the northeastern footprint and 89% for the northwestern footprint. The two rice maps were mosaicked into one. Further

details on the methodology and accuracy of the rice area maps can be found in [22]. The rice area was summarized per municipality.

3.1.2. MODIS Data Pre-Processing

Boschetti *et al.* [20] demonstrated that it is possible to identify the dates of crop establishment (transplanting or direct seeding) and heading (maximum plant development at the end of vegetative period) from time series analysis of moderate resolution EO data [20,21,28]. However, the time series data needs to be smoothed before this information can be extracted.

The synthetic 8-day time series of Terra and Aqua HDF files (See Section 0) were used to extract the necessary information to build a time series of vegetation indices and to evaluate the residual rate of noise (mainly due to residual cloud contamination) that still affected the observation after compositing. In particular, the Enhanced Vegetation Index (EVI; MOD/MYD13Q1 HDF layer 2; [29]), VI Quality information (HDF layer 3), the blue reflectance band (HDF layer 6) and the Pixel Reliability flags data (HDF layer 12) were extracted and analyzed.

EVI time series were smoothed following a two-step approach. The first step involved the detection and cleaning of outliers (*i.e.*, anomalous 'spikes') in the raw EVI profile following the approach proposed in the TIMESAT algorithm [30]. The checked EVI time series were then smoothed using a weighted Savitzky-Golay filter [31] with weights assigned on the basis of data quality. This algorithm allows data smoothing without forcing a given mathematical function (e.g., Gaussian or logistic curves) to fit the data time series thus reducing artifacts creation [31,32]. Data quality was derived from analysis of MODIS quality indicators (Pixel Reliability and VI Usefulness derived from HDF layers 12 and 3, respectively), complemented with blue reflectance data as proposed by other authors [33] (see Supplementary Table S2 for details). For each acquisition date (t), pixels (i) were classified as Clean, Contaminated or Cloudy. The Savitzky-Golay filter was then applied, using a symmetrical smoothing window of ± 3 periods, a 2nd order polynomial fitting function, and weighting EVI values of the different dates by associating them with different expected measurements errors ($Clean\ \varepsilon_t^i = 0.02; Contaminated\ \varepsilon_t^i = 0.11;\ Cloudy\ \varepsilon_t^i = 0.3$).

3.1.3. Phenological Metric Extraction from Smoothed MODIS Times Series Data

Following Boschetti *et al.* [20], a rule based method was implemented to identify the occurrence of the main phenological stages from the smoothed EVI time series. We first calculated and analyzed the derivative of the smoothed signal in order to identify all the points of local (relative) minima and local (relative) maxima. Following Manfron *et al.* [21], these minima and maxima were then evaluated with agronomically based criteria to identify which ones correspond to the transplanting and heading dates, respectively.

The transplanting dates were assumed to correspond to the local minima followed by a rapid and strong increase of the EVI smoothed signal (a sequence of at least three positive derivative points in a temporal window of five composites). The heading dates were assumed to correspond to the absolute maxima of the curve satisfying the following criteria:

i) located between 56 and 120 days after the estimated transplanting date, based on known durations of vegetative stages of rice crops grown in this area and season;
ii) showing an EVI value greater than 0.4; and
iii) followed by a rapid reduction of EVI (a decrease of 1/3 of max-EVI value within 40 days) following [21].

3.1.4. Spatial and Statistical Analysis of the Phenology Metrics

Several steps were taken to ensure that the crop status information extracted from the phenological metrics was both robust and representative.

Firstly, phenological analysis was performed only on MODIS pixels identified as rice by the SAR rice crop mask. The "detection rate" of the algorithm was analyzed for each municipality by comparing the total number of 250 m "rice pixels", derived resampling the high resolution SAR map, with the number of pixels for which the algorithm estimated the transplanting and heading dates. The phenological stages estimated from the MODIS time series were compared to crop stage information from the field. Due to the small dimension of the fields, which were selected for the analysis of VHR SAR data [22], it was not possible to perform a direct field to pixel comparison. Instead, transplanting and heading dates from MODIS were summarized at municipal level and their statistical distributions were compared against the distribution of field observed dates.

Secondly, we identified and removed unreliable estimates. We calculated the confidence intervals of the average heading occurrence in each municipality using a bootstrapping method for non-normally distributed data [34]. Municipalities where half the width of the confidence interval was greater than 8 days (*i.e.*, corresponding to the MODIS composite time span) exhibited phenological estimates with high variance due to a noisy and scattered sample and were discarded from the analysis. Additionally, any municipality with 10 or fewer pixels with heading estimates was also discarded from the analysis.

3.1.5. Indicator of Risk of Standing Rice Crop Loss from a Typhoon

The final step in the proactive assessment estimates the risk of standing rice crop loss from a typhoon with an indicator that identifies which areas of Leyte were more likely to have been impacted by the typhoon. The time span (Δ_{doy}, in days) between the estimated heading date and the typhoon occurrence was calculated for each pixel. Since harvesting can only start at the end of the ripening phase, which in the tropics occurs 30 to 40 days after heading [35], areas characterized by rice crop with a detected heading close to the typhoon event (Δ_{doy} of 30–50 days) were considered to be at risk of rice production loss due to the typhoon. The average number of days between heading and typhoon Haiyan was summarized per municipality.

Not all MODIS pixels in the rice area will meet the criteria in Section 3.1.2 for phenological metric extraction. Thus, to estimate the total rice area potentially subject to production loss, we multiplied the area of MODIS pixels with a given Δ_{doy} value by the MODIS detection rate, for each possible Δ_{doy} (Equation (1)).

$$S_{rice}(\Delta_{doy}) = S_M(\Delta_{doy}) \times DR = N_M(\Delta_{doy}) \times S_{pixel} \times DR \quad (1)$$

where $S_{rice}(\Delta_{doy})$ is the estimate of total rice area with a given Δ_{doy}, $S_M(\Delta_{doy})$ is the area of MODIS pixels with a given Δ_{doy} (computed as the product of the number of pixels $N_M(\Delta_{doy})$ by the surface of a MODIS pixel), and DR is the MODIS detection rate.

The rice area potentially subject to production loss was summarized per municipality.

3.2. Reactive Assessment of Rice Crop Damage

The reactive damage estimate is based on a simple spatial analysis of pixels classified as rice (Section 3.1.1) and as being flooded due to the typhoon. The flood detection relies on change detection applied to SAR images pre- and post-event. The relevant images for flood mapping are: 8 and 11 November (flooded images); and 16 November and 20 September (reference or non-flooded images). Because the scenes on 8 and 16 November were acquired with a different geometry, they were filtered using the single-date Gamma distribution entropy maximum *a-posteriori* method (a different method to the filtering used for the multi-date time series in [22] but all other processing to derive terrain geocoded and calibrated images were as in [22].

Flooded areas were detected with a rule-based classifier applied to the backscatter (or σ°) pixel values in the terrain geocoded and calibrated images.

1. σ^0 value for the flooded date (*i.e.*, 11 or 8 November) is less than −13 dB; this value is associated with surface water for X-band, HH data at this incidence angle as described in [22].
2. σ^0 ratio between the reference or non-flooded images and the corresponding flooded acquisitions, is larger than 2.0; this represents a strong backscatter decrease over a short period of time that is not consistent with normal rice crop practices in this region and season.

The flood damaged rice area was summarized per municipality.

4. Results and Discussion

We focus on the results of the proactive approach but place the results in context with the flooded rice area estimates from the reactive approach. We split the results into four sections. We first visually demonstrate the results of the phenological stage detection algorithm using two exemplar pixels in the study area. This is followed by an assessment of the representativeness of the detection across the entire study area. We then assess the accuracy of the detection by comparing the detected phenological stages against field observations. Finally, we estimate the standing rice crop area at risk of damage from typhoon related flooding and relate this to the flood affected area.

4.1. Example Rice Crop Phenological Stages from MODIS Time Series Data

Figure 5 shows an example for one pixel in Kananga municipality in Northwest Leyte (Figure 5a) and Pastrana municipality in Northeast Leyte (Figure 5b). The figure shows the 8-day raw EVI data (thin gray line), the effect of the smoothing process (green line), the date of landfall of the typhoon (blue diamond), the detection of transplanting date (red point), and the heading occurrence (dark-green point). The temporal profile extracted in Kananga (Figure 5a detected two seasons. In particular, the wet season, the one closer to the typhoon event, shows a rice crop establishment with transplanting at the beginning of June (DOY 153) and a peak EVI (*i.e.*, heading [20]) in late July (DOY 209). On the other hand, the

time series analyzed in Pastrana. Figure 5b clearly shows a delayed crop establishment in the wet season with rice transplanting in late July (DOY 201) and a crop peak in late September (DOY 265). The preceding dry season (from January to May) was not detected as rice due to an anomalous and slow decreasing senescence period that does not match with the expected rice behavior and time series analysis criteria [21])

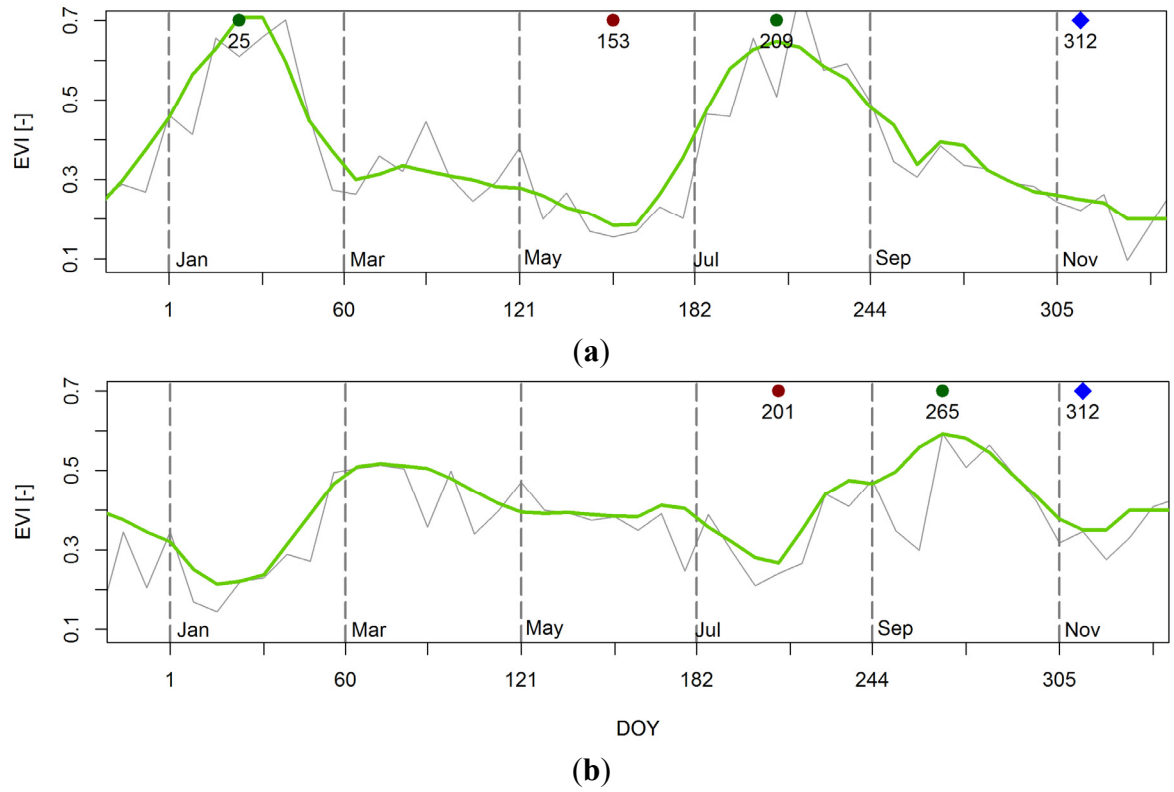

Figure 5. Time series analysis of EVI for a pixel located in the municipality of Kananga (**a**); 11°9.875′N 124°30.631′E) and Pastrana (**b**); 11°14.375′N 124°51.303′E) showing differences in planting dates during the wet season. The graphs show raw (thin black line) and smoothed EVI (green line); detected transplanting date (red point), heading occurrence (green point) and the typhoon Haiyan (blue diamond) together with their date of occurrence in DOY. Y-axis is EVI [–] and X-axis is time in DOY.

4.2. Analysis of Detection Rate

The phenological detection algorithm estimated the transplanting and heading dates for about 1700 MODIS pixels; more than 30% of the 250 m pixels in the SAR rice area. Across the study site the detection rate varied between 8% and 57%, and was found to be greater than 10% in the majority of the municipalities analyzed (21 out of 29). The detection rate is generally lower in areas characterized by low rice presence where the rice growing areas are more fragmented (low resolution bias) [36].

Figure 6 is a scatterplot of the number of rice pixels per municipality at 250 m resolution rescaled from the SAR derived rice map and the number of MODIS detected pixels per municipality. Figure 6 shows that the method provided automatic phenological estimation for a number of MODIS pixels that is proportional to the rice area in each analyzed administrative unit.

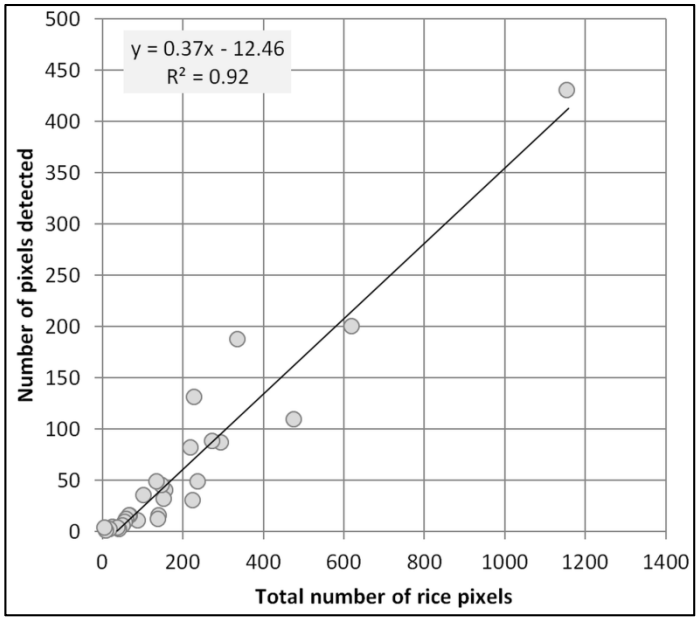

Figure 6. The relationship between the number of MODIS pixels where rice phenological dates were retrieved and the corresponding SAR derived rice area resampled at MODIS resolution in each municipality.

4.3. Analysis of Transplanting and Heading Date Accuracy

Eleven municipalities with small areas planted to rice and less than 10 MODIS pixel detections were excluded. The 18 retained municipalities account for 89% of the total rice cultivated area in the 2013 wet season and are uniformly distributed over the study area.

The box plots in Figure 7 show the estimated transplanting dates (a) and heading dates (b) derived from MODIS data for the main rice growing municipalities in Leyte. Box plots in the graph are colored in light and dark grey to highlight northwestern and northeastern municipalities, respectively, with the average longitude of the municipality increasing from left to right. The red dashed horizontal lines indicate the average transplanting and heading dates for the entire study area. Field data acquired in eight of the municipalities are also reported as colored points. Red points report the exact date recorded by ground observations. Blue points are cases where field observations did not explicitly provide the heading and the date was estimated based on crop growth stages observed across several field observations days through the season.

A *point in pixel* validation of MODIS estimated dates was not possible due to the small size of the fields with respect to MODIS spatial resolution. Instead, field observations are reported in this figure as a qualitative reference for the evaluation of the capability of the remote sensing method to identify crop establishment variability in time and space for a wide area.

Figure 7a shows how the method is able to identify variation in the timing of crop establishment within and among municipalities. Estimated dates were within reasonable agreement with field observations. Satellite estimates for transplanting fall in the expected range of dates for the study area: between May and August (DOY 120–240) with a mean value (red dotted line) in June (DOY 170). The estimates in the northwest municipalities (Kananga, Matag-Ob and Ormoc City) have earlier estimated transplanting dates (DOY 150–175) than those in the northeast (DOY 180–200), which is confirmed by

field observations. In Figure 7b it is clear that satellite estimates of heading date show a better agreement with field observations confirming that the detection of peak of season date from time series analysis is more robust than that of crop establishment [20]. Figure 7b shows the same longitudinal trend identified in Figure 7a, with heading dates in northeastern municipalities occurring around 20 days later than in northwestern ones.

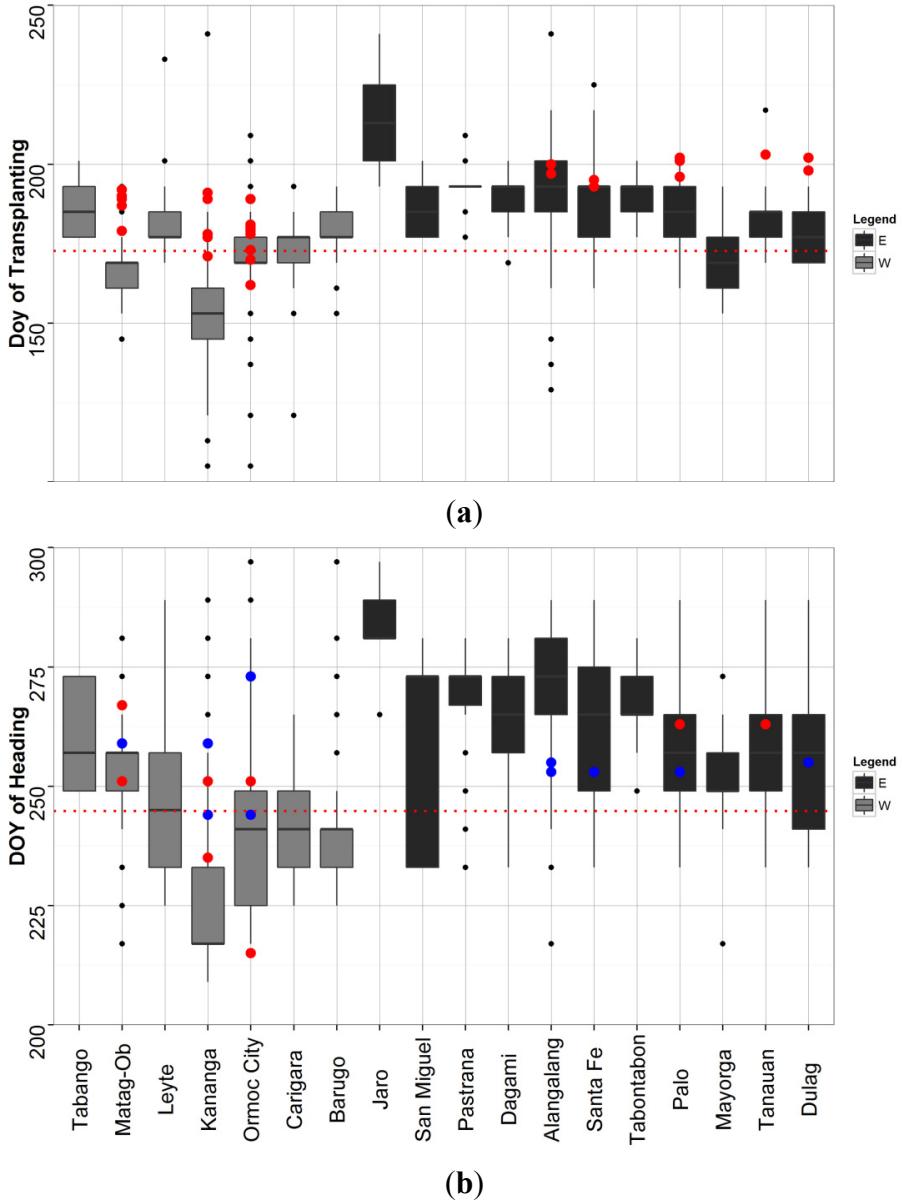

Figure 7. Box plots of the transplanting (**a**) and heading (**b**) dates in 18 municipalities for the 2013 wet season as derived from MODIS data. Red and blue points refer to observed and estimated field dates, respectively. Red dotted line represents the average value for the entire study area. Municipalities are reported from west (Tabango) to east (Dulag).

Not all monitored fields in northeast Leyte had reached the heading stage by the last in-season field visit (24 September 2013). This is also reflected in the farmer declarations of harvesting, whereby 10 out of 20 monitored fields in the northeastern footprint were not harvested before the typhoon event (See Supplementary Figure S1 and Table S1).

This qualitative assessment confirms that this approach can highlight spatial differences in agricultural practices (late and early cultivation) and plant development (variety crop cycle).

4.4. Standing Crop Area at Risk

Figure 8 provides a synthesis of the remote sensing and spatial analyses conducted in northern Leyte for the 2013 wet season.

Figure 8a,b show the high resolution rice map and flooding map from SAR, respectively, which are the basis of the accurate rice area estimation and typhoon damage estimation. Figure 8c,d show the same data aggregated to municipal area totals. Figure 8d shows that about 6500 ha were flooded and that Tanauan was the most affected municipality (1545 ha, or 24% of the total flooded area) followed by Alangalang (938 ha, or 14% of the total flooded area).

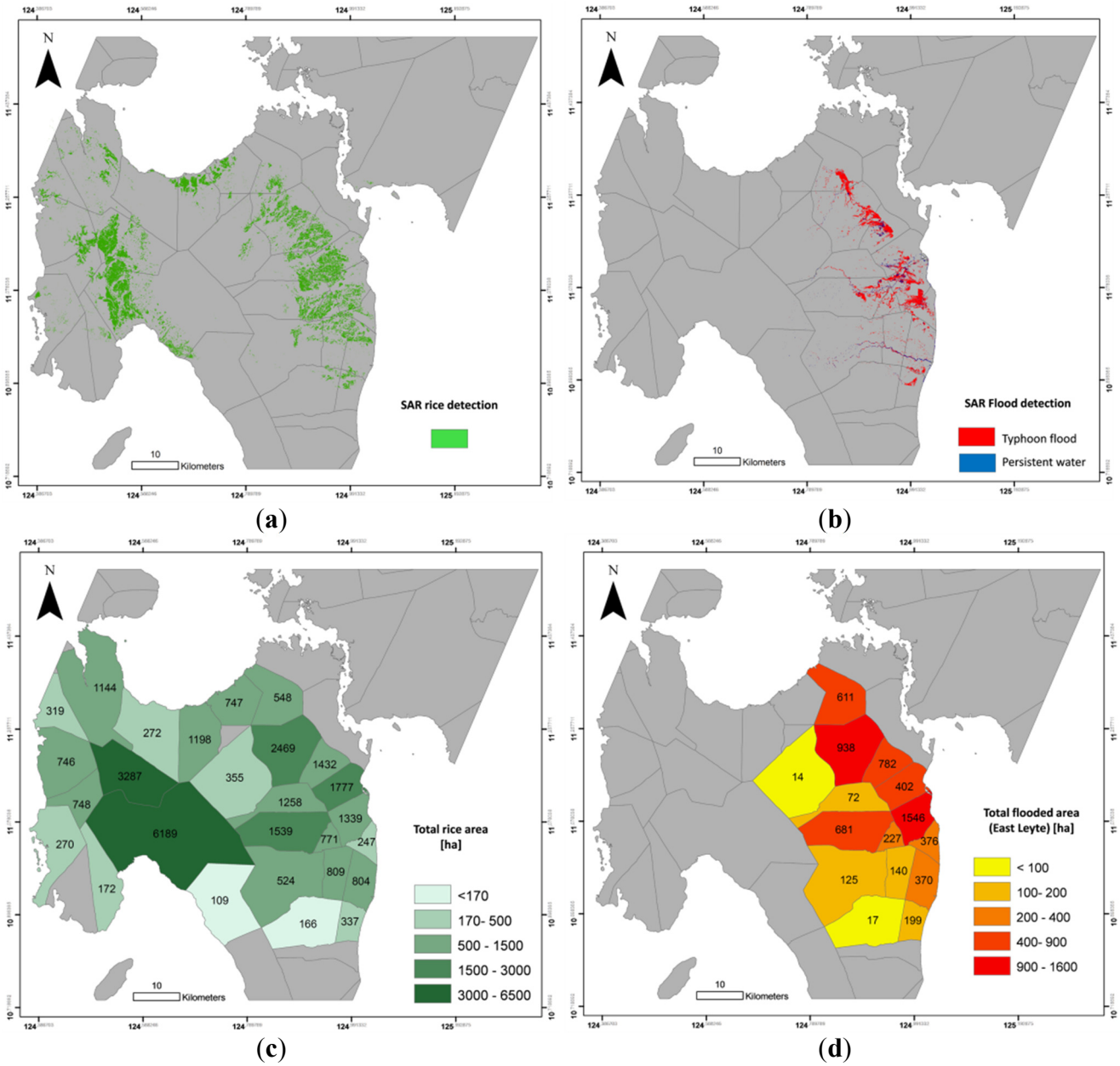

Figure 8. *Cont.*

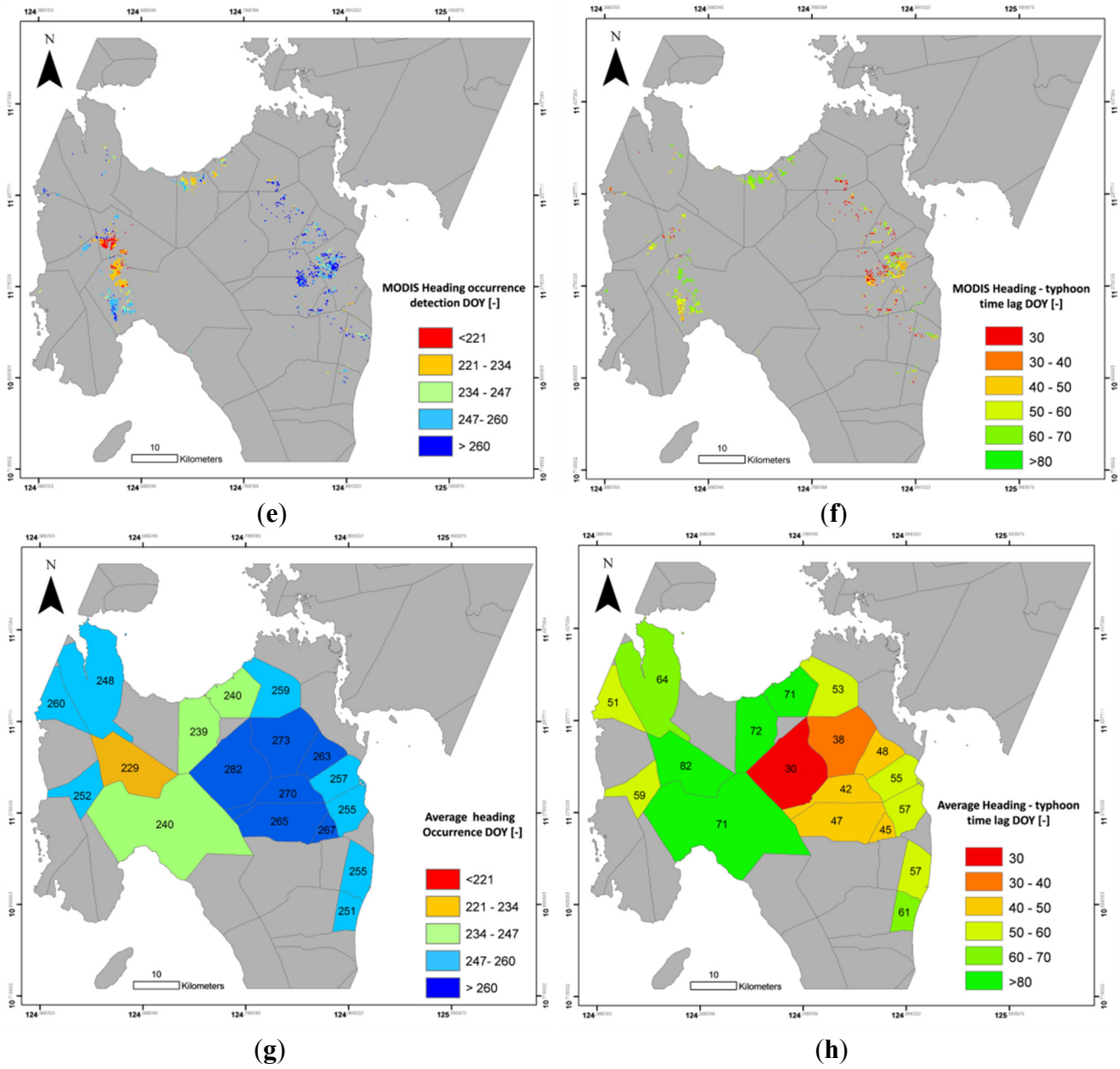

Figure 8. (**a**) Rice cultivated area from SAR; (**b**) flooded area from SAR; (**c**) rice area per municipality; (**d**) flooded area per municipality; (**e**) heading dates from MODIS; (**f**) days between heading and typhoon Haiyan per MODIS pixel; (**g**) averaged MODIS heading dates per municipality; and (**h**) average number of days between heading and typhoon Haiyan.

Figure 8e shows the MODIS derived heading date and Figure 8f shows the difference in days between heading date and the day typhoon Haiyan made landfall in Leyte (8 November). Figure 8g and Figure 8h are the same data averaged to municipal level. Gray municipalities indicate areas with no rice according to the SAR rice area map or municipalities excluded from the analysis because the criteria for selection of robust phenological estimation were not satisfied (see Section 3.1.4). Figures 8e,g provide a spatial confirmation of the results in Figure 7; rice transplanting took place later in northeastern Leyte (DOY 161–225) than in northwestern Leyte (DOY 137–201) by an average of 24 days, a substantial duration relative to the maturity of the dominant rice varieties (110–114 days). The effect of this late transplanting in the northeast is highlighted in Figures 8f and 8h, where there are fewer days between

heading and the typhoon than in the northwest. On average MODIS estimated heading dates in the northeastern municipalities occurred less than 50 days before the typhoon struck.

Overall, the panels in Figure 8 show that rice grown in northeastern Leyte was most affected by flooding due to typhoon Haiyan and at the same time those rice areas were less advanced in the rice season, thus exposing more of the standing crop to typhoon related damage.

Figure 9 shows the rice cultivated area grouped as a function of the time between the MODIS estimated heading date and the typhoon date (see Section 3.1.5). We identified two critical periods: from Typhoon (T) to T minus 30 days (T-30), where rice in the field was not yet mature, and from T minus 30 to T minus 50 days (T-50), where harvesting activities were probably not yet performed according to common practices in the area.

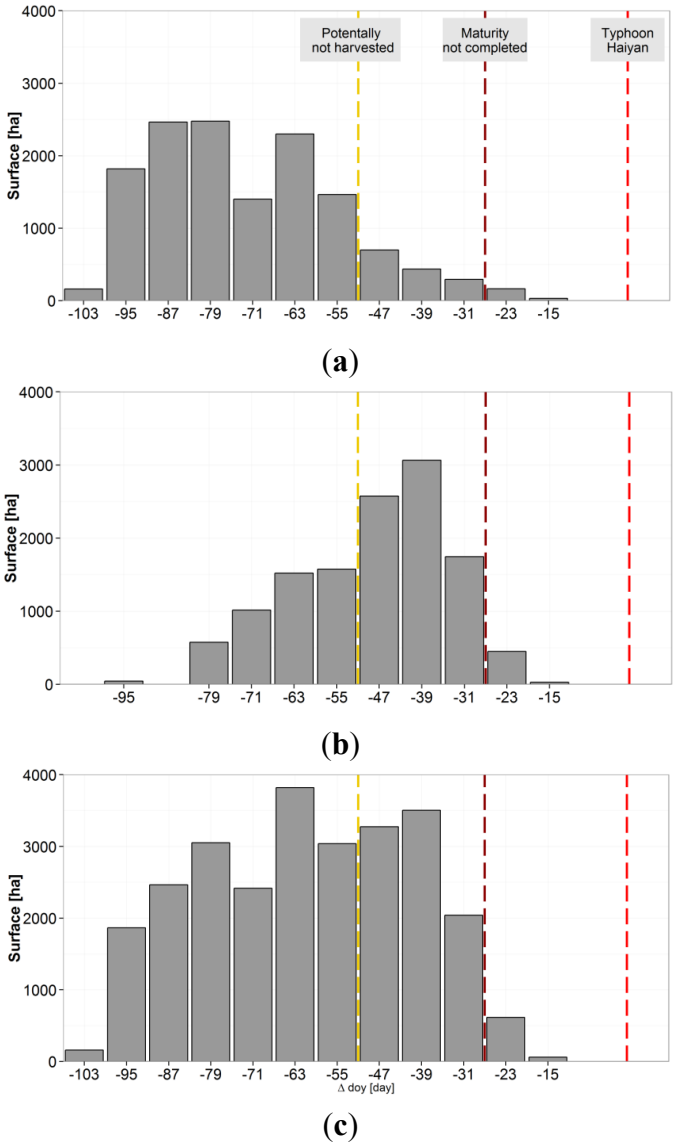

Figure 9. Distribution of rice area by time span (Δ_{doy} − in days) between the MODIS estimated heading date and the typhoon occurrence in Leyte for the 2013 wet season. Northwestern and northeastern rice areas are reported in panels (**a**) and (**b**), respectively. Panel (**c**) provides the results for the entire study area. Vertical dashed lines are 30 (brown) and 50 (yellow) days before the typhoon date (red line).

Figure 9a,b highlight that the distribution of potentially affected areas is not homogeneous between northeast and northwest Leyte. For northwest Leyte, only 1% of the rice cultivated area (corresponding to about 200 ha) was estimated not to have reached maturity at the time of the typhoon event and only 10% (corresponding to about 1400 ha) were probably not yet harvested. Conversely in northeast Leyte, about 4% of the rice cultivated area (corresponding to about 500 ha) was estimated not to have reached maturity and about 59% (corresponding to about 7000 ha) was estimated not to have been harvested yet.

The analysis highlights a much higher exposure of standing rice crop in northeastern Leyte to typhoon Haiyan. Conversely, rice production in northwestern Leyte was much less affected. This kind of assessment can provide valuable information for mitigation and disaster response strategies. Moreover, it could be used as an important (although 'qualitative') basis in the analysis of crop damage reports coming from the different parts of the province. One caveat is that the assessment is a conservative evaluation of potential production loss, due to the exclusion of some administrative units for which no reliable MODIS estimation was available.

4.5. A Proposal for an Operational Monitoring System

Rice is the most important food security crop in Asia and the major rice-growing season is particularly prone to tropical storm related losses that are likely to increase in intensity and frequency in a changing climate. Unbiased and transparent approaches to crop damage assessments are essential to reduce moral hazard and to guide appropriate investments that mitigate risk and respond to disasters. The results of this *ex-post* analysis suggest that it is feasible to provide near real time information about crop status before a tropical storm event. The fundamental aspects of the proposed system are (i) the existence of a reliable seasonal crop map; and (ii) the availability of methods able to handle hyper-temporal optical data to derive periodic crop status information. A robust proactive operational system should be able to provide crop status information regularly at specific time steps by analyzing the continuous change of temporal signal as soon as a new image is provided (e.g., [37]). The new generation of operational SAR and optical satellite mission, such as the European Sentinel program, will contribute to the necessary EO data flow to support the proposed approach. At the time of writing, the first operational Sentinel-1 SAR images are already being provided to users, while the MODIS platform, and new PROBA-V and the foreseen Sentinel-3 satellites are the best option to perform near real time agricultural monitoring and derivation of crop status condition.

5. Conclusions

This research is a contribution to literature on crop damage assessments from natural disasters. Our innovation has been the development of a proactive assessment of the risk of damage that exploit the synergy of different satellite sensors: all weather capacity of very high resolution SAR sensor are fundamental to properly map rice crop in tropical area and hypertemporal information from moderate resolution optical sensor are the only way to perform an operation crop seasonal monitoring to retrieve reliable phenological and crop practices information on large areas.

We have demonstrated a method that:

i) Can provide automatic phenological estimation using vegetation index time series derived from MODIS for a representative sample of MODIS pixels.
ii) Is conservative yet captures rice crop status information on an area that is proportional to the rice area.
iii) Can highlight spatial differences in agricultural practices and plant development.
iv) Can be used to monitor the crop in-season and provide timely information on rice crop status.

Our test case confirmed that northeastern Leyte was identified as the region most at risk to storm related damage to the standing rice crop due to the confluence of a late established rice crop in the part of the province most affected by the typhoon.

This approach can provide unbiased and transparent pre-event information that is complementary to post-event damage assessments that characterize the majority of previous studies. Ongoing and new satellite platforms can provide the required information on seasonal rice crop area, cropping calendars, crop status and area affected by typhoon related damage.

Acknowledgments

This work has been undertaken within the framework of the Remote Sensing based Information and Insurance for Crops in Emerging economies (RIICE) project financially supported by the Swiss Agency for Development and Cooperation (SDC) and by the Philippine Rice Information System (PRiSM) project funded by the Philippine Department of Agriculture—Bureau of Agricultural Research (DA-BAR). It was also supported by the CGIAR Global Rice Science Partnership (GRISP) program and the European Union Seventh Framework Programme (FP7-SPACE/2007-2013) project ERMES (grant agreement n° 606983). The authors are grateful to Raffaele Argiento for help provided in the statistical analysis. Satellite data were provided by ASI/e-GEOS from COSMO-SkyMed satellites.

Author Contributions

Conceived and designed the experiments: M.B., A.N. Performed the experiments: M.B., F.N., G.M. Analyzed SAR data: M.Ba., F.H., J.V.R. Provided field data: M.R.O.M., A.P.B., E.J.P.Q. Analyzed and interpreted the results: M.B., A.N., F.N., L.B., A.L. Wrote the paper: M.B., A.N., F.N., L.B., F.H., A.L.

Conflicts of Interest

The authors declare no conflict of interest.

References

1. Global Rice Science Partnership (GRiSP). *Rice Almanac*; 4th ed.; International Rice Research Institute: Los Banos, Philippines, 2013; p. 283.
2. Statistics Division of the Food and Agriculture Organization of the United Nations (FAOSTAT). Avaliable online: http://faostat3.fao.org/faostat-gateway/go/to/home/E (accessed on 16 March 2015).
3. Angove, M.D.; Falvey, R.J. *Annual Tropical Cyclone Report 2011*; Joint Typhoon Warning Center: Pearl Harbor, HI, USA, 2011.

4. National Disaster Reduction and Risk Management Council (NDRRMC). NDRRMC Update: Site Rep No. 104 Effects of Typhoon "Yolanda" (HAIYAN). Available online: www.ndrrmc.gov.ph (accessed on 16 March 2015).
5. Brivio, P.A.; Colombo, R.; Maggi, M.; Tomasoni, R. Integration of remote sensing data and GIS for accurate mapping of flooded areas. *Int. J. Remote Sens.* **2002**, *23*, 429–441.
6. Schnebele, E.; Cervone, G.; Waters, N. Road assessment after flood events using non-authoritative data. *Nat. Hazards Earth Syst. Sci.* **2014**, *14*, 1007–1015.
7. Lee, M.-F.; Lin, T.-C.; Vadeboncoeur, M.A.; Hwong, J.-L. Remote sensing assessment of forest damage in relation to the 1996 strong typhoon Herb at Lienhuachi Experimental Forest, Taiwan. *For. Ecol. Manag.* **2008**, *255*, 3297–3306.
8. Sanyal, J.; Lu, X.X. Application of Remote Sensing in Flood Management with Special Reference to Monsoon Asia: A Review. *Nat. Hazards* **2004**, *33*, 283–301.
9. Chau, V.N.; Holland, J.; Cassells, S.; Tuohy, M. Using GIS to map impacts upon agriculture from extreme floods in Vietnam. *Appl. Geogr.* **2013**, *41*, 65–74.
10. Dahdouh-Guebas, F.; Jayatissa, L.P.; di Nitto, D.; Bosire, J.O.; Lo Seen, D.; Koedam, N. How effective were mangroves as a defence against the recent tsunami? *Curr. Biol.* **2005**, *15*, R443–R447.
11. Kamthonkiat, D.; Rodfai, C.; Saiwanrungkul, A.; Koshimura, S.; Matsuoka, M. Geoinformatics in mangrove monitoring: damage and recovery after the 2004 Indian Ocean tsunami in Phang Nga, Thailand. *Nat. Hazards Earth Syst. Sci.* **2011**, *11*, 1851–1862.
12. Belward, A.S.; Stibig, H.J.; Eva, H.; Rembold, F.; Bucha, T.; Hartley, A.; Beuchle, R.; Khudhairy, D.; Michielon, M.; Mollicone, D. Mapping severe damage to land cover following the 2004 Indian Ocean tsunami using moderate spatial resolution satellite imagery. *Int. J. Remote Sens.* **2007**, *28*, 2977–2994.
13. Chen, P.; Liew, S.C.; Kwoh, L.K. Tsunami damage assessment using high resolution satellite imagery: a case study of Aceh, Indonesia. In Proceedings of the 2005 IEEE International Geoscience and Remote Sensing Symposium, Seoul, Korea, 25–29 July 2005; pp. 1405–1408.
14. Römer, H.; Kaiser, G.; Sterr, H.; Ludwig, R. Using remote sensing to assess tsunami-induced impacts on coastal forest ecosystems at the Andaman Sea coast of Thailand. *Nat. Hazards Earth Syst. Sci.* **2010**, *10*, 729–745.
15. Römer, H.; Jeewarongkakul, J.; Kaiser, G.; Ludwig, R.; Sterr, H. Monitoring post-tsunami vegetation recovery in Phang-Nga province, Thailand, based on IKONOS imagery and field investigations—A contribution to the analysis of tsunami vulnerability of coastal ecosystems. *Int. J. Remote Sens.* **2011**, *33*, 3090–30121
16. Sirikulchayanon, P.; Sun, W.; Oyana, T.J. Assessing the impact of the 2004 tsunami on mangroves using remote sensing and GIS techniques. *Int. J. Remote Sens.* **2008**, *29*, 3553–3576.
17. Villa, P.; Boschetti, M.; Morse, J.L.; Politte, N. A multitemporal analysis of tsunami impact on coastal vegetation using remote sensing: a case study on Koh Phra Thong Island, Thailand. *Nat. Hazards* **2012**, *64*, 667–689.
18. FAO/Philippines Crop damages after Typhoon Haiyan in the Philippines. Available online: http://www.fao.org/emergencies/crisis/philippines-typhoon-haiyan/crop-damages-map/en/ (accessed on 15 March 2015).

19. Holecz, F.; Barbieri, M.; Collivignarelli; Francesco; Gatti, L.; Nelson, A.; Setiyono, T.D.; Boschetti, M.; Manfron, G.; Brivio, P.A.; *et al*. An operational remote sensing based service for rice production estimation at national scale. In Proceedings of ESA Living Planet Symposium, Edinburgh, UK, 9–11 September 2013.
20. Boschetti, M.; Stroppiana, D.; Brivio, P.A.; Bocchi, S. Multi-year monitoring of rice crop phenology through time series analysis of MODIS images. *Int. J. Remote Sens.* **2009**, *30*, 4643–4662.
21. Manfron, G.; Crema, A.; Boschetti, M.; Confalonieri, R. Testing automatic procedures to map rice area and detect phenological crop information exploiting time series analysis of remote sensed MODIS data. *Proc. SPIE* **2012**, *8531*, 85311E:1–85311E:11.
22. Nelson, A.; Setiyono, T.; Rala, A.; Quicho, E.; Raviz, J.; Abonete, P.; Maunahan, A.; Garcia, C.; Bhatti, H.; Villano, L.; *et al*. Towards an operational SAR-based rice monitoring system in Asia: Examples from 13 demonstration sites across Asia in the RIICE Project. *Remote Sens.* **2014**, *6*, 10773–10812.
23. National Statistical Coordination Board (NSCB). 2012 Full Year Official Poverty Statistics. Available online: www.nscb.gov.ph (accessed on 16 March 2015).
24. Philippine Statistical Authority CountrySTAT. Available online: http://countrystat.bas.gov.ph/ (accessed on 16 March 2015).
25. Land Processes Distributed Active Archive Centre (LP DAAC). Available online: http://e4ftl01.cr.usgs.gov/ (accessed on January 2015).
26. Von Grebmer, K.; Ringler, C.; Rosegrant, M.W.; Olofinbiyi, T.; Wiesmann, D.; Fritschel, H.; Badiane, O.; Torero, M.; Yohannes, Y.; Thompson, J.; *et al*. 2012 Global Hunger Index | International Food Policy Research Institute (IFPRI). Available online: http://www.ifpri.org/publication/2012-global-hunger-index (accessed on 16 March 2015).
27. Global Administrative Areas Database (GADM). Available online: http://www.gadm.org/ (accessed on 18 May 2015)
28. Boschetti, M.; Nelson, A.; Manfrom, G.; Brivio, P.A. An automatic approach for rice mapping in temperate region using time series of MODIS imagery: First results for Mediterranean environment. *EGU Geophys. Res. Abstr.* **2012**, *14*, EGU2012-14068-1.
29. Huete, A.; Didan, K.; Miura, T.; Rodriguez, E.P.; Gao, X.; Ferreira, L.G. Overview of the radiometric and biophysical performance of the MODIS vegetation indices. *Remote Sens. Environ.* **2002**, *83*, 195–213.
30. Jönsson, P.; Eklundh, L. TIMESAT—A program for analyzing time-series of satellite sensor data. *Comput. Geosci.* **2004**, *30*, 833–845.
31. Chen, J.; Jönsson, P.; Tamura, M.; Gu, Z.; Matsushita, B.; Eklundh, L. A simple method for reconstructing a high-quality NDVI time-series data set based on the Savitzky–Golay filter. *Remote Sens. Environ.* **2004**, *91*, 332–344.
32. White, M.A.; Nemani, R.R. Real-time monitoring and short-term forecasting of land surface phenology. *Remote Sens. Environ.* **2006**, *104*, 43–49.
33. Xiao, X.; Boles, S.; Liu, J.; Zhuang, D.; Frolking, S.; Li, C.; Salas, W.; Moore, B. Mapping paddy rice agriculture in southern China using multi-temporal MODIS images. *Remote Sens. Environ.* **2005**, *95*, 480–492.

34. Kundzewicz, Z.; Mondiale, O. *Detecting Trend and other Changes in Hydrological Data*; Zbigniew Kundzewicz, Z., Robson, A., Eds.; World Metereological Organization: Geneva, Swizerland, 2000; p. 158.
35. IRRI Growth Stages of the Rice Plant. Available online: http://www.knowledgebank.irri.org/ericeproduction/0.2._Growth_stages_of_the_rice_plant.htm (accessed on 16 March 2015).
36. Boschetti, L.; Flasse, S.P.; Brivio, P.A. Analysis of the conflict between omission and commission in low spatial resolution dichotomic thematic products: The Pareto Boundary. *Remote Sens. Environ.* **2004**, *91*, 280–292.
37. Combal, B.; Bartholomè, E. Retrieving Phenological Stages from Low Resolution Earth Observation Data. In *Remote Sensing Optical Observation of Vegetation Properties*; Maselli, F., Menenti, M., Brivio, P.A., Eds.; Research Signpost: Kerala, India, 2010; pp. 115–129.